Extreme particle acceleration at jet termination shocks

Benoît Cerutti[a,*] **and Gwenael Giacinti**[b,c]

[a]*Univ. Grenoble Alpes, CNRS, IPAG,*
38000 Grenoble, France

[b]*Tsung-Dao Lee Institute, Shanghai Jiao Tong University,*
Shanghai 201210, P. R. China

[c]*School of Physics and Astronomy, Shanghai Jiao Tong University,*
Shanghai 200240, P. R. China
E-mail: benoit.cerutti@univ-grenoble-alpes.fr,
gwenael.giacinti@sjtu.edu.cn

Giant radio lobes forming at both ends of powerful extragalactic jets are often suspected to generate and host some of the highest-energy cosmic rays in the Universe. Using particle-in-cell simulations of a magnetized relativistic jet termination shock, we show that particles are efficiently accelerated up to the confinement limit of the system provided that the global transverse structure of the jet is taken into account. A strong tangential velocity discontinuity grows between the core and the edges of the jet leading to macroscopic shear-flow particle acceleration. Energetic particles accumulate in an over-pressured and under-dense bubble near the shock front before escaping in the downstream medium via a Von Kármán vortex street. A possible observational signature of this mechanism would be the detection of an underluminous synchrotron cavity upstream of AGN jet hotspots. These results suggest that extragalactic jet termination shocks provide exquisite conditions to accelerate cosmic rays up to the highest energies.

---

*Speaker

1. Introduction

Powerful extragalactic jets, and in particular FRII type of jets, exhibit strong relativistic and collimated outflows, mostly visible in the radio band. These jets propagate on kiloparsec scales, and the location where they terminate is usually visible as bright and compact hotspots in radio (e.g., [1]), in X-rays (e.g., [2, 3]), and potentially even in the gamma-ray range [4, 5], indicating that these hotspots are sites of efficient in-situ particle acceleration. The jet-end regions are usually surrounded by giant radio bubbles, or lobes, inflated by the decelerated flow from the jet over its lifetime, and as such, lobes represent the calorimeter of the system. Thanks to their size, and their microGauss magnetic field strength, extragalactic jet hotspots and lobes are capable of confining the highest-energy cosmic rays known in the Universe [6].

The pressing question now is whether these particles can be accelerated in these environments. Because of the compactness of hotspots, these structures are often interpreted as the jet termination shock, by analogy to pulsar wind nebulae. If so, diffusive shock acceleration is the leading model for particle acceleration [7–9]. However, magnetized shocks suffer from major shortcomings in the relativistic regime: particle acceleration is slow and saturates at low energies above the bulk, even for modest upstream plasma magnetizations [10, 11]. This important conclusion stems from the small-scale nature of the plasma turbulence seeded by the Weibel instability near the shock front. This instability is efficiently quenched by the ambient mean (perpendicular) field.

Following up on our previous studies of particle acceleration at pulsar wind nebula termination shocks [12, 13], we argue that the above conclusion is not valid on system-size scales. In this work, we demonstrate that a magnetic gradient and the presence of a magnetic null along the jet axis play a crucial role in the long-term evolution of the shock structure and particle acceleration. Our findings lead us to conclude that relativistic magnetized shocks are extremely efficient particle accelerators, in contrast to the standard diffusive shock acceleration model (e.g., [14]). This proceedings paper is based on a recent study published in [15].

2. Numerical setup and results

The fact that the structure of a relativistic shock endowed with a varying upstream magnetic field should be qualitatively different than a uniform shock relies on the expected jump conditions across the shock front. Kennel & Coroniti [16] found that the Rankine-Hugoniot solution for a relativistic perpendicular shock depends on the upstream plasma magnetization, defined as,

$$\sigma = \frac{B^2}{4\pi \Gamma n m c^2},\tag{1}$$

where B is the magnetic field strength, Γ is the bulk Lorentz factor, n is the plasma density, and m is the electron mass for a pair plasma or the ion mass for an ion-electron plasma, all quantities being defined in the upstream medium. In particular, the plasma downstream 4-velocity, $U_{\rm d} = \Gamma_{\rm d} V_{\rm d}$, is given by [16]

$$\frac{U_{\rm d}^2}{c^2} = \frac{8\sigma^2 + 10\sigma + 1}{16(\sigma + 1)} + \frac{1}{16(\sigma + 1)} \left[64\sigma^2(\sigma + 1)^2 + 20\sigma(\sigma + 1) + 1\right]^{1/2}.\tag{2}$$
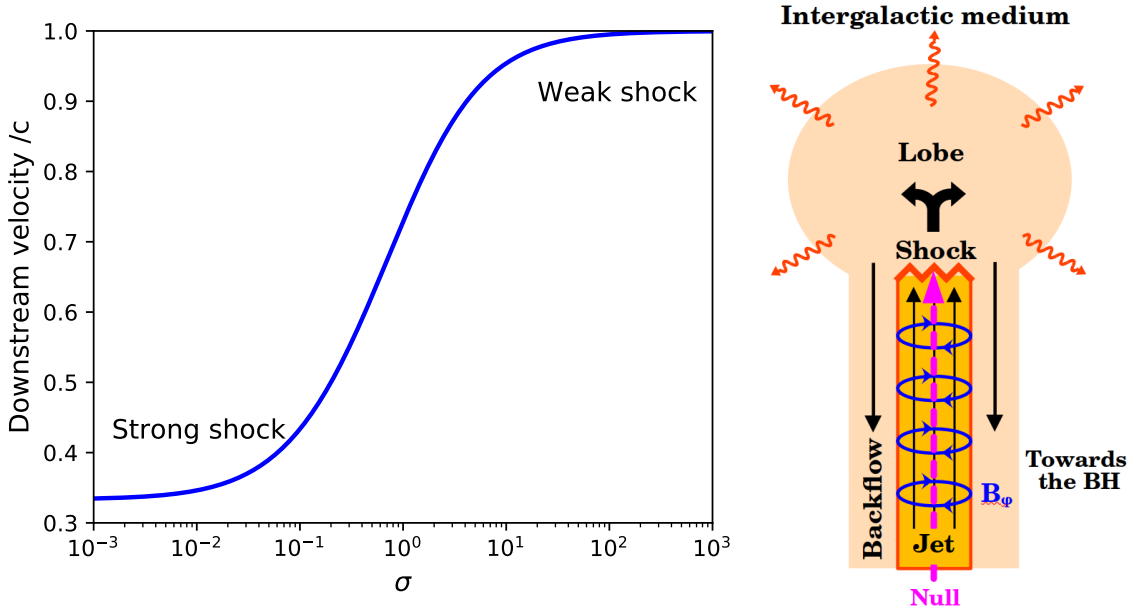
Figure 1: Left: Plasma 3-velocity downstream of a relativistic perpendicular shock as a function of the magnetization parameter, σ (see, Eq. 1), based on the Rankine-Hugoniot jump conditions (see, Eq. 2). Right: Sketch representing the overall geometry of a relativistic toroidal-dominated magnetized jet termination shock (associated to the hotspots) and decelerated flow (i.e., the lobe).

In the unmagnetized limit ($\sigma \to 0$), the shock is strong leading to a high compression of the upstream magnetic field and density in the downstream medium, and an efficient deceleration of the flow down to $V_d \to c/3$. In the high-σ limit ($\sigma \gg 1$), the compression ratio drops to the order unity and the downstream flow hardly decelerates, meaning that the shock becomes weak (see Fig. 1, left panel).

Thus, if the plasma magnetization significantly varies along the transverse direction in the upstream flow, the shock front cannot remain flat (in the plane parallel limit), and a strong velocity shear should appear in the downstream flow. The evolution of the shock as well as particle acceleration should then considerably depart from the usual uniform homogeneous shocks studied so far. The presence of a magnetic null in the system guarantees the existence of a magnetic gradient, and even, in some cases, a magnetic reversal prone to magnetic reconnection in the downstream medium [12, 13]. In the context of a relativistic jet launched by magnetic processes near the central supermassive black hole (e.g., [17, 18]), a significant toroidal field component is naturally expected, a component which, by construction, should vanish on the jet axis, representing a null line in this system. The toroidal field is then expected to grow with the distance to the jet axis (followed by a decay at the outskirts of the jet region), leading to a system-size scale gradient of the field (see Fig. 1, right panel). Powerful collimated jets, such as FR-II jets, exhibit a low degree of internal dissipation, suggesting that they may remain magnetized all the way up to the lobes.

In this work, we investigate the implication of such a large-scale magnetic field gradient in jet termination shocks, assuming that this configuration is maintained at large distances from the central engine, and that the fields and the particles are close to equipartition. To this end, we
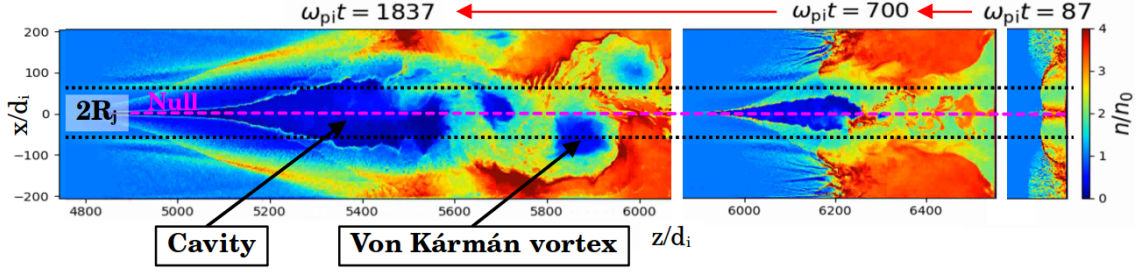
Figure 2: Time evolution (from right to left) of the plasma density at the jet termination shock, and formation of the shock front cavity and a Von Kámán vortex street in the downstream medium. Time is normalized by the inverse of the plasma frequency, ω_{pi}^{-1}, and space by the ion skindepth scale, $d_i = c/\omega_{pi}$. The jet radius, R_j, is shown by the horizontal black dotted lines. The magenta dashed line is the jet axis (i.e., the magnetic null).

performed two-dimensional particle-in-cell (PIC) simulations in a Cartesian geometry that is meant to represent a poloidal cut through a cylindral jet. We prescribe the following profile for the perpendicular magnetic field in the upstream medium,

$$B_y(x) = -\frac{B_0}{4}\left(\frac{x}{R_j}\right)\left[1 - \tanh\left(\frac{x - R_j}{\Delta}\right)\right]\left[1 + \tanh\left(\frac{x + R_j}{\Delta}\right)\right],\qquad(3)$$

where R_j is the radius of the jet, x is the coordinate across the jet in the plane of the simulation (xz-plane), while y is in the out-of-plane direction. The z-direction is defined along the jet axis. Δ defines the width of the transition layer between the magnetic jet region and the external unmagnetized medium; here it is fixed to $\Delta = 0.5R_j$. This prescription is inspired from a force-free jet solution, and it implies that the jet must be electrically charged (although quasi-neutral) and carries a net electric current in the core that is closing in the boundary layers of the jet ($|x| \gtrsim R_j$). These conditions must be matched initially in the upstream medium. The plasma is composed of electrons and ions with a mass ratio, $m_i/m_e = 25$, and it is injected with a uniform bulk Lorentz factor $\Gamma = 10$. The plasma magnetization varies from $\sigma = 0$ in the midplane to $\sigma = 1$ near the jet boundaries, $|x| = R_j$.

Figure 2 shows the time evolution of the plasma density near the shock front. In the early phases (right panel), the shock front is sharp and curved due to the varying magnetization within the jet radius as expected from the jump conditions (Eq. 2). Outside the jet radius ($|x| \gtrsim R_j$) where $\sigma \approx 0$, a standard Weibel-dominated relativistic shock forms characterized by prominent kinetic-scale filaments. At later stages (middle panel in Fig. 2), an under-dense bubble grows at the shock front in the midplane, from small scales up to the largest jet-size scales (left panel in Fig. 2). This cavity is inflated by energetic particles accelerated near the shock front. In return, the cavity effectively acts as an obstacle for the incoming flow and a strong tangential velocity shear forms on the upper and lower sides of the cavity. This double shear layer meets in the wake of the cavity leading to the formation of a Von Kámán vortex street that is well visible in the form of large bubbles trailing behind. These vortices are carved out from the shock-front cavity, taking with them energetic particles in the downstream medium away from the shock front. As a matter of fact, this process is the main escape mechanism for the high-energy particles in the system, and it regulates the size of the shock-front cavity. Vortices mix and eventually dissipate in the downstream flow, where the energetic particles can then freely escape.
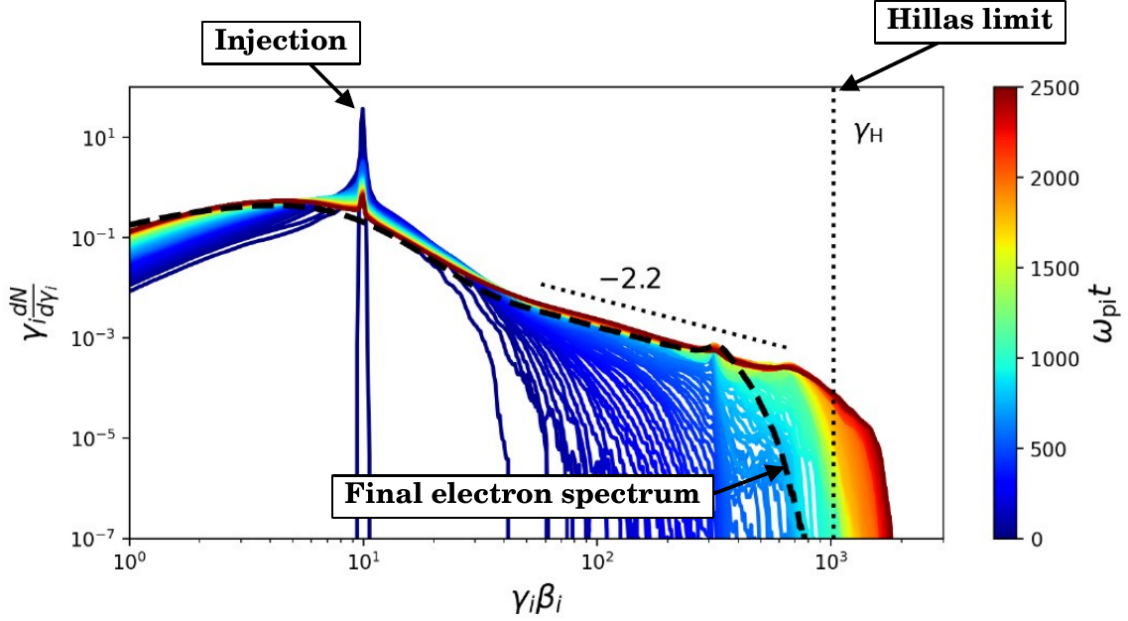
Figure 3: Time evolution (color-coded) of the ion spectrum. The final electron spectrum as a function of $\beta_e \gamma_e m_e / m_i$, where $\gamma_e = 1/\sqrt{1 - \beta_e^2}$ is the electron Lorentz factor, is shown by the black dashed line for comparison. The maximum energy set by the confinement limit of the system, γ_H, is given by the dotted vertical line. Figure adapted from [15].

Figure 3 demonstrates how efficient particle acceleration is in such a configuration. A steep ($\approx$ -2.2 slope) high-energy power-law tail grows approximately linearly with time up to the maximum energy scale that the system can confine, meaning up to the moment when the particle Larmor radius becomes comparable to the jet diameter, $\gamma_H = 2R_j e B_0 / m_i c^2 \approx 1000$ in the simulation. At this stage, the particle spectrum saturates, which corresponds to the moment when the shock-front cavity fills the entire jet radius. For comparison, the maximum particle energy reached at the same physical time in a uniform shock would be at best one order of magnitude smaller, even in the most favorable conditions of an unmagnetized shock [10]. The analysis of a large sample of high-energy particle trajectories reveals that shear-flow acceleration is at work [19, 20]. The multiple scatterings of particles across the velocity shear layers at the boundaries of the shock-front cavity efficiently accelerate particles. The energy gain is consistent with a Lorentz boost each time the particle is elastically scattered in a given fluid frame, akin to a second-order Fermi acceleration process.

3. Conclusion

The main conclusion of this work is that magnetized relativistic shocks are excellent accelerators, provided that there is a large-scale gradient in the upstream plasma magnetization, in the direction transverse to the shock front. This is in stark contrast with the conclusion drawn from plane-parallel uniform shock where particle acceleration is quenched. In some sense, this work underlines how crucial it is to consider the system-size scales and large-scale gradients to study particle acceleration in astrophysical flows, as opposed to the small-scale turbulence expected in diffusive shock acceleration that drastically limits the maximum particle energy [14]. Indeed, our

study reveals that the velocity shear in the downstream flow excites strong plasma turbulence (see also [21]), and leads to efficient particle acceleration up to the confinement limit of the system. Applied to the termination shock of relativistic magnetized jets, this mechanism can explain efficient in-situ acceleration observed in some AGN jet hotspots, and in principle it can accelerate ions up to the ultra-high-energy range. Another interesting application of this model is to microquasar jets, and in particular SS 433 where particles are accelerated up to PeV energies in what appears to be bright hotspots far from the central engine [22, 23]. Future work in this direction should investigate full 3D effects, the potential role of curvature-drift in particle acceleration which is neglected in this work (however, see [24]), as well as the role of the external medium.

Acknowledgments

References

[1] Hardcastle, M. J., Croston, J. H. 2020. Radio galaxies and feedback from AGN jets. New Astronomy Reviews 88, 101539.

[2] Snios, B., et al. 2020. The X-Ray Cavity Around Hotspot E in Cygnus A: Tunneled by a Deflected Jet. The Astrophysical Journal 891, 173.

[3] Thimmappa, R., Stawarz, Ł., Neilsen, J., Ostrowski, M., Reville, B. 2022. X-Ray Spectral Analysis of the Jet Termination Shock in Pictor A on Subarcsecond Scales with Chandra. The Astrophysical Journal 941, 204.

[4] Abdo, A. A., et al. 2010. Fermi Gamma-Ray Imaging of a Radio Galaxy. Science 328, 725.

[5] Ackermann, M., et al. 2016. Fermi Large Area Telescope Detection of Extended Gamma-Ray Emission from the Radio Galaxy Fornax A. The Astrophysical Journal 826, 1.

[6] Hillas, A. M. 1984. The Origin of Ultra-High-Energy Cosmic Rays. Annual Review of Astronomy and Astrophysics 22, 425.

[7] Axford, W. I., Leer, E., Skadron, G. 1977. The Acceleration of Cosmic Rays by Shock Waves. International Cosmic Ray Conference 132.

[8] Blandford, R. D., Ostriker, J. P. 1978. Particle acceleration by astrophysical shocks.. The Astrophysical Journal 221, L29.

[9] Bell, A. R. 1978. The acceleration of cosmic rays in shock fronts - I.. Monthly Notices of the Royal Astronomical Society 182, 147.

[10] Sironi, L., Spitkovsky, A., Arons, J. 2013. The Maximum Energy of Accelerated Particles in Relativistic Collisionless Shocks. The Astrophysical Journal 771, 54.

[11] Plotnikov, I., Grassi, A., Grech, M. 2018. Perpendicular relativistic shocks in magnetized pair plasma. Monthly Notices of the Royal Astronomical Society 477, 5238.

[12] Cerutti, B., Giacinti, G. 2020. A global model of particle acceleration at pulsar wind termination shocks. Astronomy & Astrophysics 642, A123.

[13] Cerutti, B., Giacinti, G. 2021. Formation of giant plasmoids at the pulsar wind termination shock: A possible origin of the inner-ring knots in the Crab Nebula. Astronomy & Astrophysics 656, A91.

[14] Bell, A. R., Araudo, A. T., Matthews, J. H., Blundell, K. M. 2018. Cosmic-ray acceleration by relativistic shocks: limits and estimates. Monthly Notices of the Royal Astronomical Society 473, 2364.

[15] Cerutti, B., Giacinti, G. 2023. Extreme ion acceleration at extragalactic jet termination shocks. Astronomy & Astrophysics 676, A23.

[16] Kennel, C. F., Coroniti, F. V. 1984. Confinement of the Crab pulsar's wind by its supernova remnant. The Astrophysical Journal 283, 694.

[17] Blandford, R. D., Znajek, R. L. 1977. Electromagnetic extraction of energy from Kerr black holes. Monthly Notices of the Royal Astronomical Society 179, 433.

[18] Blandford, R. D., Payne, D. G. 1982. Hydromagnetic flows from accretion disks and the production of radio jets. Monthly Notices of the Royal Astronomical Society 199, 883.

[19] Ostrowski, M. 1990. Diffusive acceleration of cosmic ray particles at tangential discontinuity of velocity field. Astronomy & Astrophysics 238, 435.

[20] Rieger, F. M., Duffy, P. 2004. Shear Acceleration in Relativistic Astrophysical Jets. The Astrophysical Journal 617, 155.

[21] Demidem, C., Nättilä, J., Veledina, A. 2023. Relativistic Collisionless Shocks in Inhomogeneous Magnetized Plasmas. The Astrophysical Journal Letters 947, L10.

[22] Abeysekara, A. U., et al. 2018. Very-high-energy particle acceleration powered by the jets of the microquasar SS 433. Nature 562, 7725.

[23] H. E. S. S. Collaboration. 2024. Acceleration and transport of relativistic electrons in the jets of the microquasar SS 433. Science 383, 6681.

[24] Huang, Z.-Q., Reville, B., Kirk, J. G., Giacinti, G. 2023. Prospects for ultra-high-energy particle acceleration at relativistic shocks. Monthly Notices of the Royal Astronomical Society 522, 4955.